Supporting Information

Continuous Magnetic Separation Microfluidic Chip for Tumor Cell *in vivo* Detection

Man Tang,[†a,b] *Jiao Feng,*[†a] *Hou-Fu Xia,*[c] *Chun-Miao Xu,*[a] *Ling-Ling Wu,*[a] *Min Wu,*[c] *Shao-Li Hong,*[a] *Gang Chen,*[*c] *Zhi-Ling Zhang*[*a]

[a] College of Chemistry and Molecular Sciences, Wuhan University, Wuhan 430072, P. R. China. Email: zlzhang@whu.edu.cn;

[b] School of Electronic and Electrical Engineering, Wuhan Textile University, Wuhan 430200, P. R. China.

[C]The State Key Laboratory Breeding Base of Basic Science of Stomatology (Hubei-MOST) and Key Laboratory of Oral Biomedicine of Ministry of Education, School and Hospital of Stomatology, Wuhan University, Wuhan 430079, P. R. China. Email: geraldchan@whu.edu.cn.

† These authors contributed equally to this work.

Table of Contents

S.1 Reagents and Instruments.

The microfluidic chip was fabricated by soft lithography technology. Related reagents include indium tin oxide glass (ITO glass, the resistance is about 10 Ω, purchased from LaiBao Hi-Tech Co., Ltd., China), the positive photoresists AZ 9260 (purchased from AZ Electronic Materials Corp.), the negative photoresists SU8-2015 (purchased from Kayaku Advanced Materials, Inc.), and the polydimethylsiloxane (PDMS, purchased from Dow Corning, USA). All the mask used in the experiments was produced in Shanghai KaiSheng Electronic. Co. Ltd., China.

The magnetic microbeads were prepared according to our previous work. Related reagents include branched poly(ethylene imine) (PEI, M.W. 25 kDa and M.W. 750 kDa,), polyvinylpyrrolidone (PVP-k30), (3-aminopropyl) triethoxysilane (APTES), *N*-(3-Dimethylaminopropyl)-*N*'-ethyl carbodiimide hydrochloride (EDC), *N*-hydroxysuccinimide (NHS), 4,6-diamidino-2-phenylindole (DAPI), bovine serum albumin (BSA), Tween-20 and anti-EpCAM monoclonal antibodies, all these reagents were purchased from Sigma-Aldrich.

The cells used in this work including Breast cancer MCF-7 cell, SK-BR-3 cell, and MDA-MB-453 cells, hepatoma carcinoma Hep G2 cell, and human peripheral blood leukemia Jurkat T cell were purchased from China Type Culture Collection. Human blood samples were supplied by the Hospital of Stomatology, Wuhan University. All the media for cell culture were bought from Gibco Corp. Isoflurane was bought from RWD Life Science Corp., and heparin sodium was got from Sinopharm Chemical Reagent Co., Ltd.

Fluorescence images were captured by a CCD camera mounted on an inverted fluorescence microscope (Ti-U, Nikon, Japan). Dynamic light scattering (DLS) was performed on a Malvern Zetasizer Nano ZS instrument. The small animal anesthesia machine was purchased from RWD Life Science Corp., and the peristaltic pump (Masterflex C/L) was bought from Cole-Parmer China.

S.2 Fabrication and experimental details

S.2.1 Magnetic Nanoparticles Preparation and Modification

The magnetic nanoparticles (MNs) and fluorescent-magnetic nanoparticles (FMNs) were prepared according to our published work about the layer-by-layer (LBL) assembly method.[1] Five layers of nano-γ-Fe_2O_3 were coated on the surface of the Pst-AAm-COOH nanospheres to prepare MNs. FMNs were composed of four layers of nano-γ-Fe_2O_3 and three layers of quantum dot (with emission of 605 nm). For further use in CTC capture, the prepared MNs were modified with anti-EpCAM antibodies by carbodiimide chemistry (IMNs). The resulting IMNs were stored in 1% hydroxypropyl methylcellulose (HPMC) for later use.

S.2.2 Microfluidic Chip Design and Fabrication

The design of the continuous magnetic separation microfluidic chip was performed on AutoCAD. The fabrication method for the chip was mainly soft lithography as in our previous work.[2, 3] Thereinto, to fabricate the nickel wire, ITO glass with conductive properties was applied instead of conventional glass slide for electroplating. The thickness of the nickel pattern was about 12 μm and the width of each nickel wire was 50 μm. On the other side, the height of the microfluidic channel was about 57 μm, and the heights of the buffer area and reaction area were both 70 μm.

The length and width of the microfluidic channel in the magnetic lateral migrant area, reaction area, and magnetic recovery area were 13 mm×0.8 mm, 20 mm×7 mm, and 15 mm ×0.6 mm, respectively. For balancing the hydraulic pressure in the microfluidic chip, there was a microchannel was set with a length and width of 11 mm×0.2 mm. Besides that, the width of all the microchannels connected to the three areas was 300 μm.

S.2.3 Cell Culture

All the cancer cells (MCF-7 cell, SK-BR-3 cell, Hep G2 cell, MDA-MB-453 cell, and Jurkat T cell) used in this work were cultured in common cell culture flasks at 37 ℃ with DMEM supplemented with 10% fetal bovine serum and 100 IU/mL penicillin-streptomycin in a humidified atmosphere with 5% CO_2 (in the air). For better distinction, cells were stained with DAPI and DiI for 20 min before experiments. Whole blood samples used in this work were collected from healthy volunteers into an EDTA-coated vacutainer tube and were used within 24 h. All the cell lines used in this work were purchased from the China Center for Type Culture Collection.

S.2.4 Ex vivo CTC detection

The inner wall of the continuous magnetic separation chip was treated with 1% BSA and 0.1% Tween-20 for 20 min before the experiment. Then blood sample and the IMNs (with a concentration of 2 mg/mL) were separately introduced into the chip from the two inlets (inlet I and inlet II) with a flow rate

of 20 μL/min. The PBS was also introduced into the chip from Inlet III, and the captured CTCs were collected from Outlet II, while the blood sample would return to the mouse from Outlet III at the same time. The numbers of captured and uncaptured MCF-7 cells were recorded to evaluate the cell capture efficiencies. The magnetic nanoparticle separation efficiency was calculated by measuring the absorbance of the collected and original magnetic nanoparticle solution.

S.2.5 In vivo CTC monitor

Five to eight weeks C57BL/6 mice (BALB/c background) were purchased from Hunan SJA Laboratory Animal Co., Ltd. All animal experiments were performed according to protocols approved by Animal Using Protocol of the Animal Experiment Center of Wuhan University. The mouse was hocussed and limb fixed during the whole process of the *in vivo* experiment. The connection between the microfluidic chip and the mouse was a polyethylene tube with an inner diameter of about 0.28 mm, and the flow of the blood was controlled by a peristaltic pump. To prevent blood clotting, all the microchannels and the tubes were rinsed with heparin sodium (1 mg/mL) solution three times before use.

For better observation, about 10^5 MCF-7 cells which were stained by DAPI for cell nuclear and DiI for cytomembrane were injected into the mouse through the jugular catheter. Then the blood was extracted from the other jugular catheter and introduced into the continuous magnetic separation microfluidic chip. Right after that, the tumor cell in the living animal was collected and the number of the tumor cell was recorded every minute after the injection.

S.3 Modification of the IMNs

Before experiments, the prepared MNs should be modified by the antibody, so that the tumor cells can be captured by the IMNs in the microfluidic chip. In this work, the surface of the MNs is rich in carboxyl groups so the antibody can be modified on the surface of MNs by condensation reaction. To verify the modification, Cy3-labeled rabbit anti-mouse IgG was used to react with the IMNs. As shown in **Figure S1**, almost all the antibody-modified magnetic nanoparticle shows a fluorescence signal while nearly no fluorescence can be found on the unmodified MNs. These results confirmed that the modified IMNs kept active and could be applied to the following experiment.

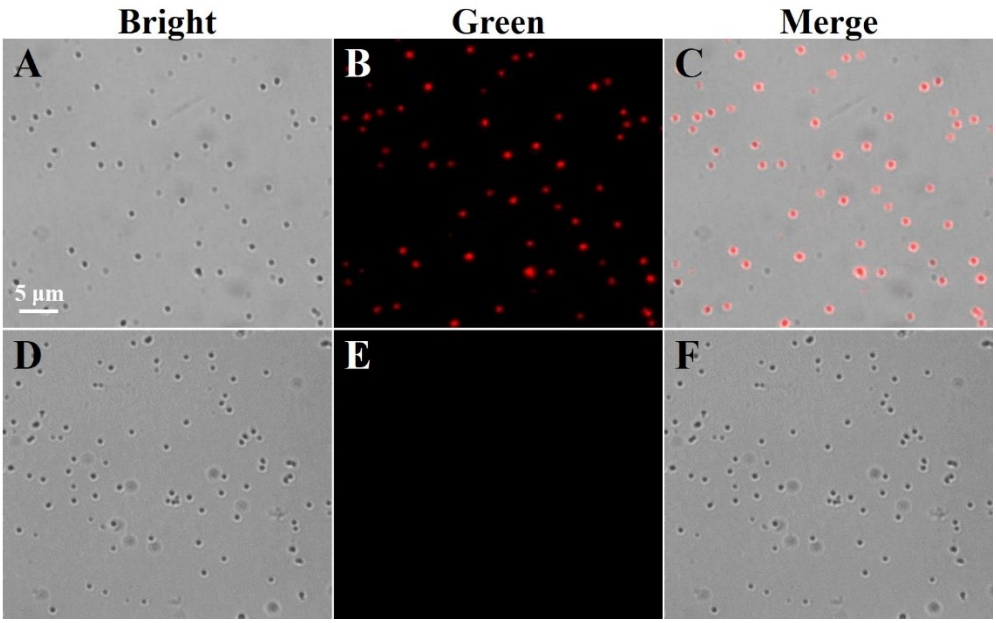

Figure S1 Bright image, fluorescence image, and merge image of the IMNs (A-C) and MNs (D-F) after reaction with Cy3-labeled rabbit anti-mouse IgG. Cy3: excitation 550 nm, emission 570 nm bandpass.

S.4 Structure of the Continuous Magnetic Separation Microfluidic Chip

The design of the continuous magnetic separation microfluidic chip was performed on AutoCAD. In this study, nickel wires are electroplated on the ITO glass of its conductivity. This fabrication process combines soft lithography and electroplating, which is time-consuming. To simplify the fabrication process, the reusability of the chip is desired. Therefore, a thin layer of PDMS film was spin-coated on the ITO glass, thus the nickel wires are encapsulated in the ITO glass. Subsequently, a microfluidic channel made of PDMS was bonded on it for further experiments. After the experiment, the microfluidic channel with the PDMS thin film can be torn down and the ITO glass with nickel wire can be retained to be reused.

To verify the function of the magnetic separation chip, the fluorescent magnetic nanoparticles (FMNs) which consist of four layers of nano-γ-Fe_2O_3 and three layers of quantum dot (with emission at 605 nm) were applied. As shown in **Figure S2A**, a stable laminar flow formed at the beginning of the microfluidic channel of the magnetic lateral migrant area. While under the function of the external magnetic, the FMNs are laterally migrated into the blood sample without any aggregation. Then as shown in **Figure S2B**, FMNs uniformly dispersed in the whole reaction area in a laminar flow manner. No obvious agglomeration between the FMNs could be observed along the sample flow, which is beneficial for subsequent tumor cell capture. Finally, almost all the FMNs were transferred to the buffer with the help of nickel wire and the function of the magnetic field in the recovery area. The above results confirmed that our designed magnetic separation chip could regulate and control the motion of magnetic nanoparticles accurately, which served as an important basis for tumor cell detection and in vivo CTC monitoring by this continuous magnetic separation microfluidic chip.

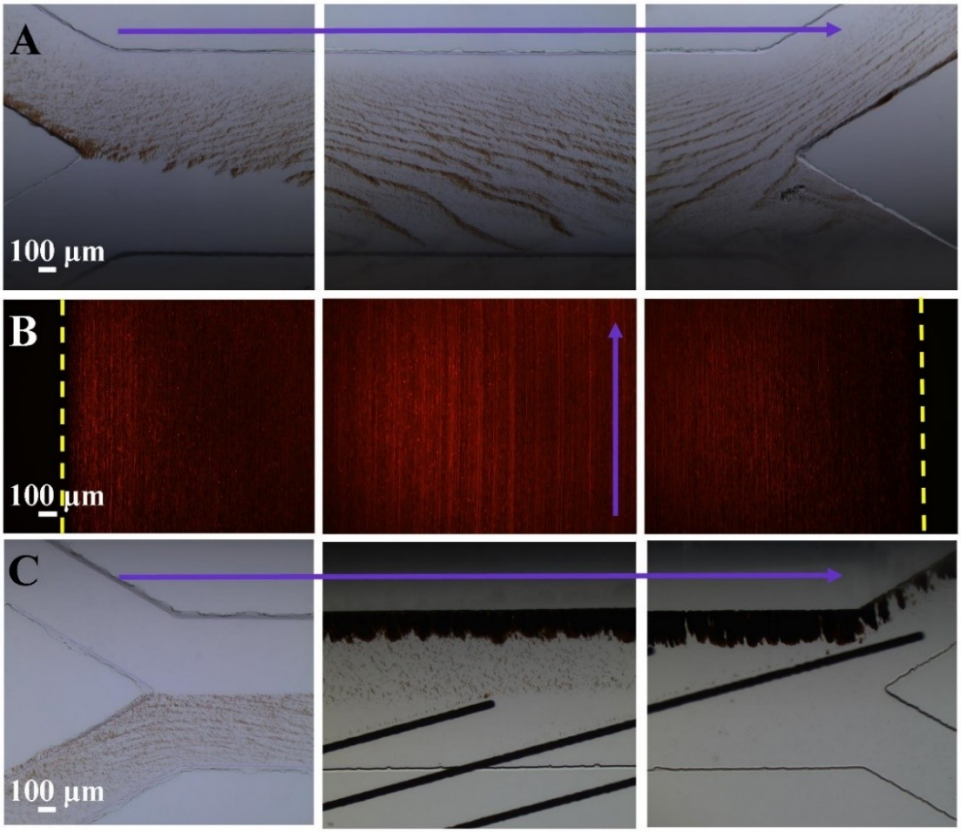

Figure S2 Characterization of the performance of the magnetic separation microfluidic chip. (A) Bright images of the FMNs motion path in the magnetic lateral migrant area. (B) Fluorescence images of the FMNs distribution in the reaction area. (C) Bright images of the FMNs motion path in the magnetic recovery area with nickel wires. The purple arrow shows the direction of the flow.

S.5 Optimization of the Continuous Magnetic Separation Microfluidic Chip

Flow rate is a critical parameter for cell capture in microfluidic devices, and it is usually optimized first. To keep the laminar effect, the introduced flow rates for the sample (DAPI-stained MCF-7 cells) and IMN were kept consistent in this work. The flow rates of 15 μL/min, 18 μL/min, 20 μL/min, 25 μL/min, and 30 μL/min were set to investigate their influence on capture efficiency. The cell capture efficiency was present by the ratio of the captured tumor cell number to the total number of introduced tumor cells. **Figure S3A** showed that the capture efficiency of the tumor cells keeps over 90% when the flow rate was in the range of 15-20 μL/min. Further increasing the flow rate decreased the capture efficiency. Whereas, cell capture efficiency could still maintain up to 80% when the flow rate was 30 μL/min, showing this continuous magnetic separation microfluidic chip had a wide flow rate range and high throughput for tumor cell capture.

To ensure sufficient contact between the IMNs and the tumor cells in the blood, two reaction areas were established. Tumor cell capture efficiency was mainly determined by the probability of contact between tumor cells and IMNs. Hence, in this continuous magnetic separation microfluidic chip, the width and the height of the reaction area were two main factors to improve the tumor cell capture efficiency. To control the variables, the widths of the microfluidic channel in the two reaction areas were fixed, while the heights of the two reaction areas were optimized. Five kinds of reaction areas whose height was 35 μm, 40 μm, 60 μm, 70 μm, and 90 μm were designed. As shown in **Figure S3B**, the tumor cell capture efficiency increased rapidly at first and then decreased slightly upon raising the height of the reaction area. Reaction area with a height below 60 μm afforded tumor cell capture efficiency of less than 70%, which could be ascribed to the insufficient interaction between IMNs and tumor cells. The slight decrease in the cell capture efficiency in the reaction area with a height of 90 μm was partially due to the sedimentation or loss of tumor cells and magnetic nanoparticles. To prevent cell sedimentation and maintain the high throughput, a flow rate of 20 μL/min and an optimal reaction area height of 70 μm were used in the subsequent experiments.

Due to its high permeability, nickel was an ideal material to enhance the local magnetic field in the recovery area. Thereinto, the placement of the nickel wire affects the magnetic force of the magnetically tagged tumor cells, hence the angle of the nickel wire relative to the horizontal line was optimized. In this work, several 30 μm wide and 7 mm long nickel wires were set under the microfluidic channel, and their gap was set as 200 μm to avoid IMN accumulation. To evaluate the separation efficiency of the continuous magnetic separation microfluidic chip, the MNs capture efficiency was calculated by the ratio of the concentration of the separated MNs solution to the concentration of the original MNs solution. Results were shown in **Figure S3C**, both the separation efficiencies of MNs and magnetically tagged MCF-7 cells with nickel wires were higher than that without nickel wires, showing that nickel wire was helpful

to improve the separation efficiency of magnetic materials. Moreover, with the increase of the angle between the nickel wire and the horizontal direction, the capture efficiencies of the magnetically tagged MCF-7 cells and IMNs were gradually improved. It was also remarkable that the separation efficiency of magnetic nanoparticles is 98.5±0.3% when the angle of the nickel wire was 12°, which was an important guarantee for biosafety in the following *in vivo* experiments. In conclusion, the angle of the nickel wire of 12° was chosen to be the optimal condition for the following experiments.

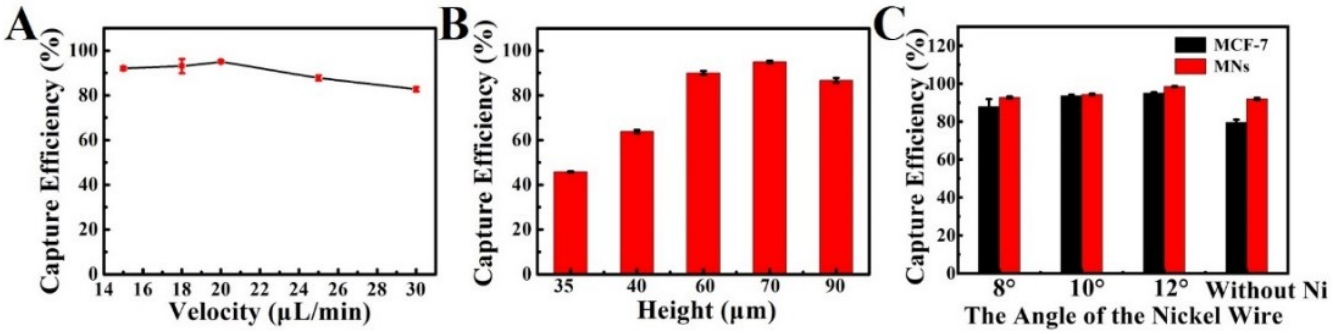

Figure S3. (A) The relationship between the flow rates of the introduced MCF-7 cells and capture efficiencies. (B) The relationship between the heights in the mixing area and capture efficiencies towards MCF-7 cells. (C) The relationship between the angle of the nickel wires in the recovery area and capture efficiencies towards MNs and MCF-7 cells. The error bars indicate the standard deviation of three experiments.

S.6 Fabrication of the Single-Cell Array Microfluidic Chip

The single-cell array microfluidic chip is fabricated by a standard soft lithography method reported in our previous work.[4, 5] Firstly the template was made on a silicon wafer with SU8-2015, and the height of each array was about 25 μm. Then the PDMS prepolymer was poured on the silicon wafer and baked for solidification. After peeling and putting on a piece of glass, the single-cell array was formed on the PDMS, and then it can be bonded with the microfluidic channel by oxygen plasma. Thus, the single-cell array microfluidic chip was obtained and can be used for cell analysis and identification.

The single-cell array contains hundreds of micropillars made by the PDMS. The micropillar is a semicircular cylinder in shape with a slit whose width is decreased from 20 μm to 8 μm gradually (**Figure S4**). The recovered tumor cells would be trapped in the single-cell array based on their size and deformability. While the excess unreacted magnetic nanoparticles flowed away.

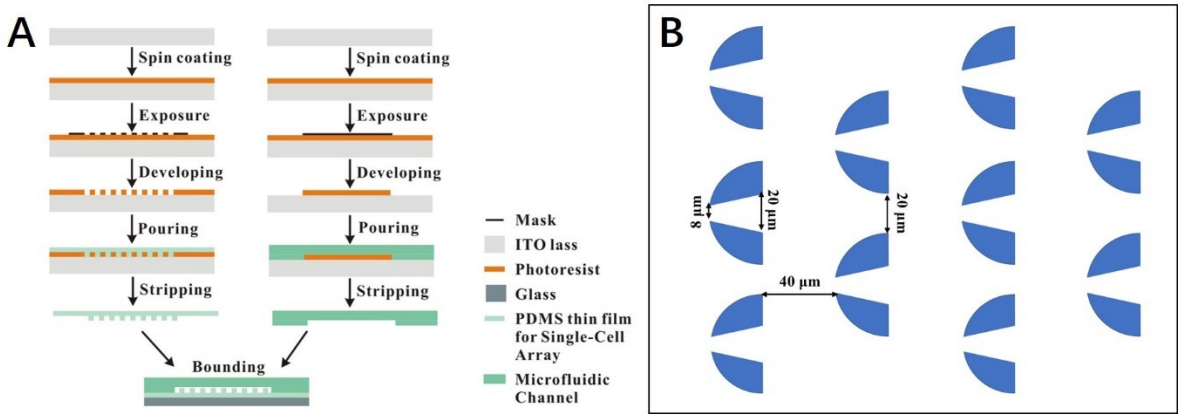

Figure S4 Design of the single-cell array microfluidic chip. (A) Schematic diagram of the fabrication process of the single-cell array microfluidic chip (B) Schematic structure of the single-cell array microfludic chip.

S.7 Identification of the Captured Tumor Cells in the Single-Cell Array Chip.

As shown in **Figure S5,** this chip effectively removed almost all the excess unreacted magnetic nanoparticles, which ensured the following cell identification. Besides, statistics indicate that about (93.26 ± 0.67)% of cells were alive after magnetic separation, and (90.48 ± 2.77)% of cells were still active even after forming a single-cell array. **Figure S5** also verified that the captured tumor cells could be purified and further used for three-color immunocytochemistry ICC identification. These results confirmed that both the continuous magnetic separation chip and the single-cell array microfluidic chip had little effect on cell activity and phenotype, which was beneficial for the subsequent cell analysis.

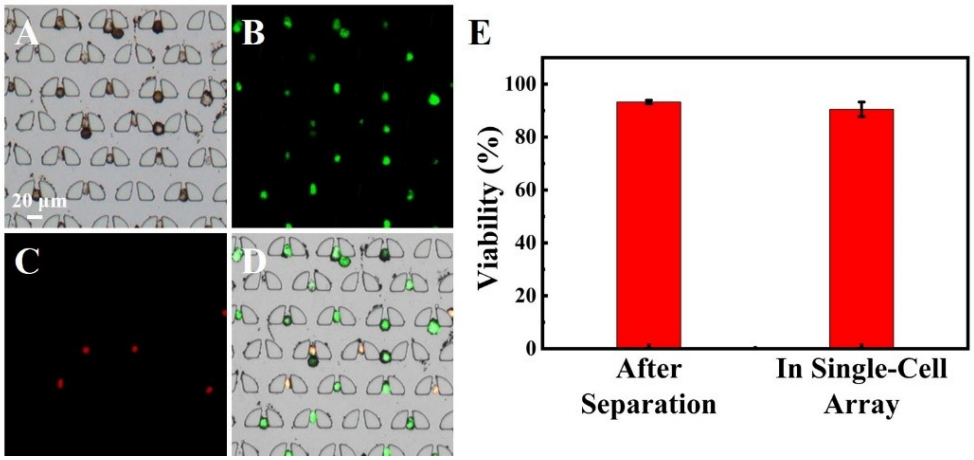

Figure S5. Viability characterizations of the captured MCF 7 cells. (A-D) Fluorescence microscopy images of the captured cells stained with Calcein AM (green, live) and PI (red, dead) in the single-cell pattern chip. (E) Viability efficiency of the captured tumor cells after being separated by the continuous magnetic chip and after trapping in the single-cell array chip respectively. The error bars indicate the standard deviation of three experiments.

The captured cells can be identified by using this single-cell array microfluidic chip with the three-color ICC identification. After forming the single cell array, the captured cells were successively reacted with DAPI (blue, a kind of nuclear staining), fluorescein isothiocyanate (FITC)-labeled anti-Cytokeratin 19 (CK19, green, a marker for epithelial cells), and allophycocyanin (APC)-labeled anti-CD45 (red, leukocyte common antigen-antibody). CTCs were defined as DAPI+, CK-19+, and CD45- with sizes up to 10 μm, and the white blood cells were DAPI+, CK-19-, and CD45+ with sizes down to 15 μm. As is indicated in **Figure S6,** taking advantage of this single-cell array microfluidic chip, not only the excess magnetic nanoparticle can be removed, but most of the blood cells are also excluded. In this way, the purity of the captured CTCs is significantly enhanced, and the identification results are simple and easy to distinguish.

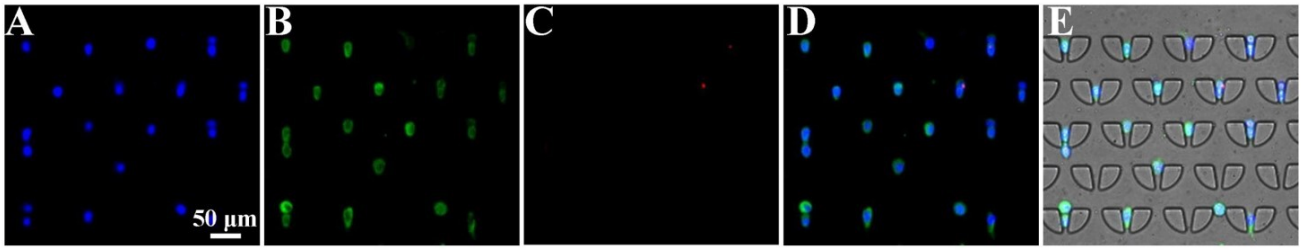

Figure S6 Microscopic images of the captured MCF 7 cells in a single-cell pattern chip and the cells were identified with the three-color ICC identification. Nucleus (DAPI): excitation 405 nm, emission 447 ± 30 nm bandpass. CK 19 (FITC): excitation 488 nm, emission 525 nm bandpass. CD45 (PE): excitation 488 nm, emission 575 nm bandpass. Merge: merge image of the nucleus (DAPI), CK 19 (FITC), and CD45 PE.

References

1. C.-Y. Wen, L.-L. Wu, Z.-L. Zhang, Y.-L. Liu, S.-Z. Wei, J. Hu, M. Tang, E.-Z. Sun, Y.-P. Gong, J. Yu and D.-W. Pang, *ACS Nano*, 2014, **8**, 941-949.
2. M. Tang, C.-Y. Wen, L.-L. Wu, S.-L. Hong, J. Hu, C.-M. Xu, D.-W. Pang and Z.-L. Zhang, *Lab Chip*, 2016, **16**, 1214-1223.
3. P. L. Guo, M. Tang, S. L. Hong, X. Yu, D. W. Pang and Z. L. Zhang, *Biosens. Bioelectron.*, 2015, **74**, 628-636.
4. L. L. Wu, M. Tang, Z. L. Zhang, C. B. Qi, J. Hu, X. Y. Ma and D. W. Pang, *Anal. Chem.*, 2018, **90**, 10518-10526.
5. L. L. Wu, Z. L. Zhang, M. Tang, D. L. Zhu, X. J. Dong, J. Hu, C. B. Qi, H. W. Tang and D. W. Pang, *Angew. Chem. Int. Ed. Engl.*, 2020, **59**, 11240-11244.